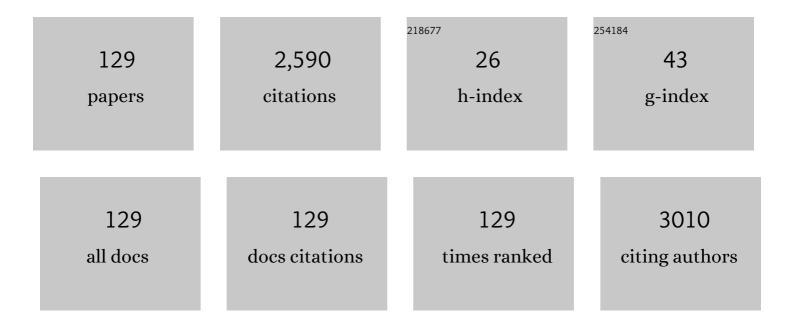
List of Publications by Year in descending order

Source: https://exaly.com/author-pdf/6468454/publications.pdf Version: 2024-02-01



#	Article	IF	CITATIONS
1	Lightweight and Resilient ZrO ₂ –TiO ₂ Fiber Sponges with Layered Structure for Thermal Insulation. Advanced Engineering Materials, 2022, 24, .	3.5	18
2	Effect of high-pressure vapor on the microstructure and mechanical properties of TiO2 continuous fibers. Ceramics International, 2022, 48, 10659-10666.	4.8	3
3	Electrospun flexible calcium zirconate fiber membrane with excellent thermal stability and alkali resistance. Ceramics International, 2022, 48, 12408-12414.	4.8	9
4	Modification of YSZ fiber composites by Al2TiO5 fibers for high thermal shock resistance. Journal of Advanced Ceramics, 2022, 11, 922-934.	17.4	23
5	Water-stable metal–organic framework (UiO-66) supported on zirconia nanofibers membrane for the dynamic removal of tetracycline and arsenic from water. Applied Surface Science, 2022, 596, 153559.	6.1	19
6	Strong Flexible Ceramic Nanofiber Membranes for Ultrafast Separation of Oil Pollutants. ACS Applied Nano Materials, 2022, 5, 9389-9400.	5.0	7
7	High-temperature flexible, strength and hydrophobic YSZ/SiO2 nanofibrous membranes with excellent thermal insulation. Journal of the European Ceramic Society, 2021, 41, 1471-1480.	5.7	51
8	Electrospun lanthanum-doped barium titanate ceramic fibers with excellent dielectric performance. Materials Characterization, 2021, 172, 110859.	4.4	11
9	Effects of the atmosphere on the high tensile strength and robust flexibility of Lu2O3 fibrous membrane. Ceramics International, 2021, 47, 8382-8388.	4.8	4
10	Self-supporting super hydrophilic MgFe2O4 flexible fibers for Pb(II) adsorption. Separation and Purification Technology, 2021, 266, 118584.	7.9	13
11	High temperature and high strength Y2Zr2O7 flexible fibrous membrane for efficient heat insulation and acoustic absorption. Chemical Engineering Journal, 2021, 416, 128994.	12.7	46
12	Preparation and excellent dielectric properties of flexible Ba0.7Sr0.29La0.01TiO3 composite fiber ceramics. Journal of Materials Science: Materials in Electronics, 2021, 32, 26359-26370.	2.2	0
13	Efficient removal of phosphate from aqueous solution by mesoporous Zr/La hydroxide fibers prepared with high-pressure steam heat treatment. Journal of Environmental Chemical Engineering, 2021, 9, 106697.	6.7	5
14	Preparation and fine thermal insulation performance of Gd2Zr2O7/ZrO2 composite fibers. Ceramics International, 2020, 46, 1615-1620.	4.8	8
15	Electrospun SiO2-MgO hybrid fibers for heavy metal removal: Characterization and adsorption study of Pb(II) and Cu(II). Journal of Hazardous Materials, 2020, 381, 120974.	12.4	85
16	Electrospinning fabrication of flexible Fe3O4 fibers by sol-gel method with high saturation magnetization for heavy metal adsorption. Materials and Design, 2020, 186, 108298.	7.0	42
17	Zirconia/polyethylene terephthalate ceramic fiber paper separator for high-safety lithium-ion battery. Ionics, 2020, 26, 6057-6067.	2.4	10
18	Preparation of mesoporous zirconia ceramic fibers modified by dual surfactants and their phosphate adsorption characteristics. Ceramics International, 2020, 46, 14019-14029.	4.8	15

#	Article	IF	CITATIONS
19	Citric-acid-assisted sol-gel synthesis of mesoporous silicon-magnesium oxide ceramic fibers and their adsorption characteristics. Ceramics International, 2020, 46, 10105-10114.	4.8	14
20	High-Efficient Photocatalytic Performance under Visible Light of Functionalized TiO ₂ Nanofibers via Steam and Pressure Co-Modification. Journal of Physical Chemistry C, 2019, 123, 17306-17317.	3.1	11
21	Preparation, mechanical properties, and diffuse reflectance of YAG continuous fibers and nanofibers. Ceramics International, 2019, 45, 21213-21219.	4.8	13
22	Flexible TiO2 ceramic fibers near-infrared reflective membrane fabricated by electrospinning. Ceramics International, 2019, 45, 6959-6965.	4.8	19
23	Controllable synthesis of Ag/AgCl@MIL-88A <i>via in situ</i> growth method for morphology-dependent photocatalytic performance. Journal of Materials Chemistry C, 2019, 7, 5451-5460.	5.5	33
24	Effect of La2O3 on Grain Refinement and Thermal Conductivity of 6 mol % Y2O3–ZrO2 Fibers. Russian Journal of Inorganic Chemistry, 2019, 64, 1464-1468.	1.3	2
25	Improved preparation of electrospun MgO ceramic fibers with mesoporous structure and the adsorption properties for lead and cadmium. Ceramics International, 2019, 45, 3743-3753.	4.8	36
26	Zirconia fiber membranes based on PVDF as high-safety separators for lithium-ion batteries using a papermaking method. Journal of Solid State Electrochemistry, 2019, 23, 269-276.	2.5	18
27	Template-free synthesis of MgO mesoporous nanofibers with superior adsorption for fluoride and Congo red. Ceramics International, 2018, 44, 9454-9462.	4.8	42
28	Photocatalytic selective hydroxylation of phenol to dihydroxybenzene by BiOI/TiO2 p-n heterojunction photocatalysts for enhanced photocatalytic activity. Applied Surface Science, 2018, 439, 1047-1056.	6.1	77
29	Effects of cerium addition on the microstructure, mechanical properties and thermal conductivity of YSZ fibers. Ceramics International, 2018, 44, 7077-7083.	4.8	10
30	Tubular structure TiO2/C/TiO2 hybrid derived from the waste of the fluff of chinar tree. Journal of Alloys and Compounds, 2018, 737, 774-789.	5.5	11
31	Effects of water vapor on the crystallization and microstructure manipulation of MgO ceramic fibers. Ceramics International, 2018, 44, 5257-5265.	4.8	6
32	Water steam modified crystallization and microstructure of mesoporous TiO2 nanofibers. Ceramics International, 2018, 44, 2158-2164.	4.8	15
33	Electrospun mesoporous zirconia ceramic fibers for catalyst supporting applications. Ceramics International, 2018, 44, 282-289.	4.8	29
34	Hierarchically Microâ€∤Nanostructured TiO ₂ /Micron Carbon Fibers Composites for Longâ€Life and Fastâ€Charging Lithiumâ€Ion Batteries. ChemElectroChem, 2018, 5, 540-545.	3.4	13
35	Characterization and adsorption mechanism of ZrO2 mesoporous fibers for health-hazardous fluoride removal. Journal of Hazardous Materials, 2018, 346, 82-92.	12.4	126
36	The influence of phosphine ligand substituted [2Fe2S] model complexes as electro-catalyst on proton reduction. RSC Advances, 2018, 8, 42262-42268.	3.6	12

#	Article	IF	CITATIONS
37	Electrospun fabrication, excellent high-temperature thermal insulation and alkali resistance performance of calcium zirconate fiber. Ceramics International, 2018, 44, 14013-14019.	4.8	20
38	Fabrication of dense and porous Li2ZrO3 nanofibers with electrospinning method. Applied Physics A: Materials Science and Processing, 2018, 124, 1.	2.3	13
39	Direct synthesis of phenol by novel [FeFe]-hydrogenase model complexes as catalysts of benzene hydroxylation with H2O2. RSC Advances, 2017, 7, 2934-2942.	3.6	30
40	Effect of the Terminal Ligands of [FeFe]â€Hydrogenase Model Complexes on Proton Reduction Properties and Catalytic Hydroxylation of Benzene. ChemistrySelect, 2017, 2, 3306-3310.	1.5	3
41	Fabrication of dense barium zirconate fibers by electrospinning with different complex agents. Journal of the American Ceramic Society, 2017, 100, 4491-4499.	3.8	9
42	Biomimetic synthesis of micro/nanostructured tubular TiO ₂ photocatalyst: adjusting the shape of the outer tube wall from nanoparticles to interlaced nanofibers and nanobelts. CrystEngComm, 2017, 19, 2312-2319.	2.6	8
43	Synthesis and electrochemical properties of [FeFe]-hydrogenase model complexes with acid-functionalized or base-functionalized ligands. Journal of Applied Electrochemistry, 2017, 47, 583-591.	2.9	Ο
44	Mesoporous ZrO 2 fibers with enhanced surface area and the application as recyclable absorbent. Applied Surface Science, 2017, 399, 288-297.	6.1	33
45	Bio-inspired Catalyst: [(μ -(SCH(CH2 CH3)CH2 S))Fe(CO)5]2 (μ,k1 ,k1 -DPPF) for Proton Reduction and Phenol Hydroxylation. ChemistrySelect, 2017, 2, 9407-9411.	1.5	4
46	High-temperature stable electrospun MgO nanofibers, formation mechanism and thermal properties. Ceramics International, 2017, 43, 16210-16216.	4.8	14
47	Enhanced photocatalytic performance of Au/TiO2 nanofibers by precisely manipulating the dosage of uniform-sized Au nanoparticles. Applied Physics A: Materials Science and Processing, 2017, 123, 1.	2.3	13
48	Polyaceticzirconium for zirconia continuous fibers: Polymeric evolution process and the relationship between polymeric structure and rheological behavior. Ceramics International, 2017, 43, 14176-14182.	4.8	12
49	Preparation of a CeO2-nanoparticle thermal radiation shield coating on ZrO2 fibers via a hydrothermal method. Ceramics International, 2017, 43, 14183-14191.	4.8	17
50	Ferrocene particles incorporated into Zr-based metal–organic frameworks for selective phenol hydroxylation to dihydroxybenzenes. RSC Advances, 2017, 7, 38691-38698.	3.6	34
51	Growth mechanism, dielectric, elastic and thermal properties of zinc cadmium thiocyanate crystal as a potential piezoelectric crystal. Chemical Physics Letters, 2017, 685, 401-409.	2.6	0
52	Large scale fabrication of magnesium oxide fibers for high temperature thermal structure applications. Ceramics International, 2017, 43, 1455-1459.	4.8	9
53	Fabrication, heat-treatment and formation mechanism of MgO fiber using propionic acid as ligand. Ceramics International, 2017, 43, 2004-2011.	4.8	13
54	Effects of atmosphere and stabilizer on the decomposition and crystallization of polyacetylacetonatozirconium. Journal of Thermal Analysis and Calorimetry, 2017, 127, 1889-1895.	3.6	16

#	Article	IF	CITATIONS
55	Formation of Barium Zirconate Fibers for Highâ€Temperature Thermal Insulation Applications. Journal of the American Ceramic Society, 2016, 99, 2913-2919.	3.8	9
56	Effects of pressure and atmosphere on the crystallization and grain refinement of zirconia fibers. Ceramics International, 2016, 42, 14189-14195.	4.8	9
57	Synthesis, structural characterization, and chemical properties of pentacoordinate model complexes for the active site of [Fe]-hydrogenase. RSC Advances, 2016, 6, 84139-84148.	3.6	7
58	Electrochemical catalysis investigation into the dynamic coordination properties of a pyridine-substituted [2Fe2S] model complex. International Journal of Hydrogen Energy, 2016, 41, 22991-22996.	7.1	9
59	Fabrication of La2Zr2O7 ceramic fibers via electrospinning method using different La2O3 precursors. Ceramics International, 2016, 42, 16633-16639.	4.8	22
60	Color tunable up-conversion emission from ZrO ₂ :Er ³⁺ ,Yb ³⁺ textile fibers. RSC Advances, 2016, 6, 103973-103980.	3.6	12
61	Biomimetic synthesis of interlaced mesh structures TiO2 nanofibers with enhanced photocatalytic activity. Journal of Alloys and Compounds, 2016, 668, 113-120.	5.5	14
62	Seedless growth of ZnO nanorods on TiO ₂ fibers by chemical bath deposition. CrystEngComm, 2016, 18, 1215-1222.	2.6	5
63	Preparation, ferromagnetic and photocatalytic performance of NiO and hollow Co3O4 fibers through centrifugal-spinning technique. Materials Research Bulletin, 2016, 74, 319-324.	5.2	16
64	Two novel polytitanium precursors containing linear Ti–(OH)2–Ti chains applied for the preparation of titanium dioxide fibers. Applied Physics A: Materials Science and Processing, 2015, 121, 723-730.	2.3	4
65	Exfoliated MoS ₂ supported Au–Pd bimetallic nanoparticles with core–shell structures and superior peroxidase-like activities. RSC Advances, 2015, 5, 10352-10357.	3.6	53
66	Titanium dioxide fibers prepared from two novel polytitanium precursors containing linear Ti–OH–Ti chains applied for photocatalytic degradation. Materials Letters, 2015, 153, 191-194.	2.6	8
67	Guanidine-phosphate non-covalent interaction in LAP crystal growth solution evidenced from spectroscopy studies. Spectrochimica Acta - Part A: Molecular and Biomolecular Spectroscopy, 2015, 148, 12-17.	3.9	2
68	Third-order nonlinearity and passive Q-switching of Cr^4+:YGG garnet crystal. Optics Letters, 2015, 40, 2421.	3.3	7
69	Rheological behavior, molecular structure of precursor and evolution mechanism: zirconia fibers from polyaceticzirconium precursors. Journal of Sol-Gel Science and Technology, 2015, 76, 482-491.	2.4	36
70	Lipase Immobilized on Graphene Oxide As Reusable Biocatalyst. Industrial & Engineering Chemistry Research, 2014, 53, 19878-19883.	3.7	44
71	Characterization and strong piezoelectric response of an organometallic nonlinear optical crystal: CdHg(SCN) ₄ (C ₂ H ₆ SO) ₂ . Journal of Materials Chemistry C, 2014, 2, 723-730.	5.5	10
72	ZnO long fibers: large scale fabrication, precursor and the transformation process, microstructure and catalytic performance. RSC Advances, 2014, 4, 57534-57540.	3.6	2

#	Article	IF	CITATIONS
73	Bulk growth and physical properties of diguanidinium phosphate monohydrate (G2HP) as a multi-functional crystal. CrystEngComm, 2014, 16, 930-938.	2.6	36
74	Crystal growth, structure and spectroscopic studies of a novel organic single crystal: Lâ€lysine pâ€nitrophenolate monohydrate (LLNP). Crystal Research and Technology, 2013, 48, 1087-1096.	1.3	11
75	Poly(amidoamine) modified graphene oxide as an efficient adsorbent for heavy metal ions. Polymer Chemistry, 2013, 4, 2164.	3.9	149
76	Magnetic dimer and tetramer based on dmit – Preparation, crystal structures, physicochemical characterization and magnetic properties. Inorganica Chimica Acta, 2013, 404, 68-76.	2.4	1
77	Studies on the conformational transformations of l-arginine molecule in aqueous solution with temperature changing by circular dichroism spectroscopy and optical rotations. Journal of Molecular Structure, 2012, 1026, 71-77.	3.6	13
78	Synthesis of partially hydrogenated graphene and brominated graphene. Journal of Materials Chemistry, 2012, 22, 15021.	6.7	93
79	A general strategy to prepare graphene-metal/metal oxide nanohybrids. Journal of Materials Chemistry, 2011, 21, 14498.	6.7	26
80	Sulfonated graphene as water-tolerant solid acid catalyst. Chemical Science, 2011, 2, 484-487.	7.4	247
81	Study on micro-crystallization, growth, optical properties and defects of a nonlinear optical crystal: MnHg(SCN)4. Journal of Crystal Growth, 2011, 317, 92-97.	1.5	12
82	Nonlinear Optical Studies of [(C ₄ H ₉) ₄ N][Ni(dmit) ₂] by Z-Scan Technique. Chinese Physics Letters, 2011, 28, 107803.	3.3	2
83	Third-order nonlinear optical properties inÂ[(C4H9)4N]2[Cu(C3S5)2]-doped PMMA thin film using Z-scan technique in picosecond pulse. Applied Physics A: Materials Science and Processing, 2010, 99, 279-284.	2.3	21
84	Investigation of the nonlinear absorption and optical limiting properties of two [Q]2[Cu(C3S5)2] compounds. Optics and Laser Technology, 2010, 42, 732-736.	4.6	20
85	INVESTIGATION OF THIRD-ORDER NONLINEAR OPTICAL PROPERTIES OF BFDT-DOPED PMMA THIN FILMS USING Z-SCAN TECHNIQUE. Modern Physics Letters B, 2009, 23, 3361-3368.	1.9	1
86	Study on nonlinear optical absorption properties of [(CH3)4N]2[Cu(dmit)2] by Z-scan technique. Optics and Laser Technology, 2009, 41, 209-212.	4.6	15
87	Distinct growth phenomenon observed on l-Arg·CF3COOH crystals. Current Applied Physics, 2009, 9, 22-25.	2.4	5
88	Fabrication of zirconia mesoporous fibers by using polyorganozirconium compound as precursor. Microporous and Mesoporous Materials, 2009, 119, 230-236.	4.4	23
89	Growth, Morphology, Thermal, Spectral, Linear, and Nonlinear Optical Properties of <scp>l</scp> -Arginine Bis(trifluoroacetate) Crystal. Crystal Growth and Design, 2009, 9, 3251-3259.	3.0	65
90	Tetraphenylphosphonium bis(2-thioxo-1,3-dithiole-4,5-dithiolato)aurate(III) acetone solvate and ethyltriphenylphosphonium bis(2-thioxo-1,3-dithiole-4,5-dithiolato)aurate(III). Acta Crystallographica Section C: Crystal Structure Communications, 2008, 64, m46-m49.	0.4	3

#	Article	IF	CITATIONS
91	Crystal growth, morphology, spectrographic characterization and thermal properties of 4,5â€bis(benzoylthio)â€1,3â€dithioleâ€2â€thione. Crystal Research and Technology, 2008, 43, 874-881.	1.3	4
92	Measurement of l-arginine trifluoroacetate crystal nucleation kinetics. Journal of Crystal Growth, 2008, 310, 2590-2592.	1.5	20
93	Nucleation growth mechanism and defects of nonlinear optical crystals of l-Arg·CF3COOH. Materials Letters, 2008, 62, 1986-1988.	2.6	7
94	Crystallization process and microstructure of sol–gel derived Pb0.9La0.1Ti0.875O3 fine fibers with a novel heat-treatment process. Solid State Sciences, 2008, 10, 859-863.	3.2	12
95	STUDY ON THIRD-ORDER OPTICAL NONLINEARITY OF BIS(TETRABUTYLAMMONIUM)-Hg(dmit)2 BY FEMTOSECOND OPTICAL KERR GATE TECHNIQUE. Modern Physics Letters B, 2008, 22, 1573-1577.	1.9	1
96	Synthesis, crystal structure and saturable absorption in the near-IR regions of a new copper complex of dmit: hexadecyltrimethylammonium <i>bis</i> (2-thioxo-1,3-dithiole-4,5-dithiolato)-copper. Journal of Coordination Chemistry, 2008, 61, 768-775.	2.2	8
97	Preparation and Property for MgB ₂ Superconductive Phase Lines Using MgH ₂ and NaBH ₄ as Starting Materials by Laser Irradiation. Japanese Journal of Applied Physics, 2008, 47, 7857.	1.5	2
98	Preparation and transmission loss of the nano-crystal and polymer composite Bi 4 Ti 3 O 12 /PEK-c films. Proceedings of SPIE, 2008, , .	0.8	0
99	Nonlinear optical studies of an organo-metallic complex by Z-scan technique. Proceedings of SPIE, 2007, , .	0.8	0
100	Atomic Force Microscopy Studies on {101} Surfaces of <scp> </scp> -arginine Trifluoroacetate Single Crystals. Journal of Physical Chemistry C, 2007, 111, 14165-14169.	3.1	10
101	Crystal growth of high quality nonlinear optical crystals of l-arginine trifluoroacetate. Journal of Crystal Growth, 2007, 308, 130-132.	1.5	24
102	Hexadecyltrimethylammonium bis(2-thioxo-1,3-dithiole-4,5-dithiolato-κ2 S 4,S 5)nickelate(III). Acta Crystallographica Section E: Structure Reports Online, 2006, 62, m757-m759.	0.2	1
103	Butyltriphenylphosphonium bis(2-thioxo-1,3-dithiole-4,5-dithiolato)nickelate(III). Acta Crystallographica Section E: Structure Reports Online, 2006, 62, m1419-m1421.	0.2	1
104	Synthesis and characterization of Co2+: MgAl2O4 nanocrystal. Journal of Sol-Gel Science and Technology, 2006, 38, 245-249.	2.4	14
105	Study on the third-order nonlinear optical properties of bis(tetrabutylammonium)bis(1,3-dithiole-2-thione-4,5-dithiolato)cadium. Optics Communications, 2005, 256, 256-260.	2.1	33
106	Preparation and optical constants of the nano-crystal and polymer composite Bi4Ti3O12/PMMA thin films. Optics and Laser Technology, 2005, 37, 259-264.	4.6	22
107	Poly[bis(N-methylformamide)tetra-μ-thiocyanato-manganese(II)mercury(II)]. Acta Crystallographica Section C: Crystal Structure Communications, 2005, 61, m278-m280.	0.4	3
108	Bis(tetraethylammonium) bis(2-thioxo-1,3-dithiole-4,5-dithiolato)cuprate(II). Acta Crystallographica Section E: Structure Reports Online, 2005, 61, m717-m719.	0.2	5

#	Article	IF	CITATIONS
109	4,5-Bis(phenylsulfonylthio)-1,3-dithiolane-2-thione. Acta Crystallographica Section E: Structure Reports Online, 2005, 61, o1432-o1433.	0.2	0
110	Bis(N-methylpyridinium) bis(2-thioxo-1,3-dithiole-4,5-dithiolato)zincate(II). Acta Crystallographica Section E: Structure Reports Online, 2005, 61, m2408-m2410.	0.2	3
111	Study on the third-order nonlinear optical properties of bis(tetraethylammonium)bis(1,3-dithiole-2-thione-4,5-dithiolato)mercury. Journal of Optics, 2005, 7, 510-513.	1.5	4
112	Edge dislocation and superstructure in MgB2superconducting crystals. Superconductor Science and Technology, 2005, 18, 1513-1516.	3.5	10
113	Physicochemical properties and theoretical explanation of ZnCd(SCN)4 crystal. Materials Research Bulletin, 2004, 39, 1407-1416.	5.2	7
114	Single crystal growth of MgB2 by using Mg-self-flux method at ambient pressure. Journal of Crystal Growth, 2004, 268, 123-127.	1.5	12
115	Growth and properties of UV nonlinear optical crystal ZnCd(SCN)4. Materials Research Bulletin, 2003, 38, 1269-1280.	5.2	19
116	The growth and properties of Ca3TaGa3Si2O14 single crystals. Journal of Crystal Growth, 2003, 253, 378-382.	1.5	31
117	Preparation and transmission loss of the nano-crystal and polymer composite film BTO/PMMA. Optics and Laser Technology, 2003, 35, 291-294.	4.6	6
118	Growth and Characterization of Series Nd:GdxLa1-xVO4 (x = 0.80, 0.60, 0.45) Crystals. Journal of Materials Research, 2002, 17, 556-562.	2.6	9
119	Crystal Growth and Characterization of a New Organometallic Nonlinear-Optical Crystal Material: MnHg(SCN)4(C3H8O2). Physica Status Solidi A, 2002, 191, 106-116.	1.7	21
120	Growth and characterization of a novel UV nonlinear optical crystal: [MnHg(SCN)4(H2O)2]·2C4H9NO. Journal of Crystal Growth, 2002, 234, 469-479.	1.5	26
121	Violet light generation by frequency doubling of GaAlAs diode laser using a metallo-organic complex crystal ZnCd(SCN)4. Optics and Laser Technology, 2001, 33, 121-124.	4.6	26
122	Crystal growth and physical properties of UV nonlinear optical crystal zinc cadmium thiocyanate, ZnCd(SCN)4. Chemical Physics Letters, 2001, 346, 393-406.	2.6	24
123	Growth of zinc cadmium thiocyanate single crystal for laser diode frequency-doubling. Journal of Crystal Growth, 2001, 222, 755-759.	1.5	21
124	Growth and properties of UV nonlinear optical crystal ZnCd(SCN)4. Materials Research Bulletin, 2001, 36, 1287-1299.	5.2	29
125	Synthesis and characterization of a new lambda-type polymer for nonlinear optics based on carbazole derivative salt. Reactive and Functional Polymers, 2000, 46, 59-65.	4.1	5
126	A novel organometallic nonlinear optical complex crystal: Cadmium mercury thiocyanate dimethyl-sulphoxide. Progress in Crystal Growth and Characterization of Materials, 2000, 40, 111-114.	4.0	8

#	Article	IF	CITATIONS
127	Growth of cadmium mercury thiocyanate dimethylsulphoxide single crystal for laser frequency doubling. Progress in Crystal Growth and Characterization of Materials, 2000, 40, 75-79.	4.0	10
128	Blue-violet light second harmonic generation with CMTC crystals. Journal of Materials Science Letters, 2000, 19, 1255-1257.	0.5	23
129	Intracavity-frequency-doubling of a 946 nm Nd:YAG laser with cadmium mercury thiocyanate crystal. Optics and Laser Technology, 1998, 30, 291-293.	4.6	13